IEEE Access
Multidisciplinary | Rapid Review | Open Access Journal

Received April 4, 2019, accepted April 23, 2019, date of publication May 7, 2019, date of current version May 23, 2019.

Digital Object Identifier 10.1109/ACCESS.2019.2915382

Over Thermal Decomposition Characteristics of $C_5F_{10}O$: An Environmental Friendly Insulation Medium

FUPING ZENG[1], ZHAOFENG WAN[1], ZHICHENG LEI[1], JU TANG[1], LIANGJUN DAI[1], XIAOHUA WANG[2], AND QIANG YAO[3]

[1]School of Electrical Engineering and Automation, Wuhan University, Wuhan 430072, China
[2]Xi'an Jiaotong University, Xi'an 710049, China
[3]State Grid Chongqing Electric Power Company Electric Power Research Institute, Chongqing 40112, China

Corresponding author: Fuping Zeng (Fuping.Zeng@whu.edu.cn)

This work was supported in part by the National Natural Science Foundation of China under Grant 51877157.

ABSTRACT $C_5F_{10}O$ gas insulating medium has attracted wide attention in the power industry for its excellent environmental potential and insulation performance. When $C_5F_{10}O$ gas is applied in power industry engineering, it will inevitably face the over thermal fault which often occurs inside the equipment. Under the long-term effect of the local over thermal fault, whether $C_5F_{10}O$ itself can maintain stability is an important factor to determine its engineering application. However, the thermal stability characteristics of $C_5F_{10}O$ and its mixture are still unknown. Therefore, through systematic experimental research on the existing experimental platform of partial over thermal of the gas insulating medium, this paper explores the initial decomposition temperature of 5% $C_5F_{10}O$ and 95% CO_2 mixture, the formation conditions of decomposition components, the relationship between the generation characteristics of decomposition components and fault temperature, and so on. The results show that when the pressure of 5% $C_5F_{10}O$ and 95% CO_2 is 0.2MPa, the mixture begins to decompose at about 400° to form C_3F_8 and C_3F_6. C_2F_6 and CF_4 will be produced at above 500°. The process of C_3F_6 formation is the endothermic reaction, while the process of C_3F_8, C_2F_6 and CF_4 formation is an exothermic reaction, which is very beneficial to the formation of C3F6 un-der superheated conditions. As a result, the product concentration shows as C_3F_6 > C_3F_8 >C_2F_6 >CF_4, and the rate of product formation is positively correlated with the over thermal fault temperature. The results of this study lay a foundation for the application of $C_5F_{10}O$ gas in the electric industry.

INDEX TERMS Environmental friendly insulating medium, $C_5F_{10}O$, thermal stability, over thermal decomposition characteristics.

I. INTRODUCTION

SF_6 has been widely used as an insulating gas with its excellent performance in various electrical insulation equipment. However, the severe greenhouse effect of SF_6 gas will have a serious impact on human atmospheric living environment [1]. The environmental problems of SF_6 have gradually become an important factor that restricts the green development of China's and even the global power grid [2]. Therefore, it is imperative to explore a new alternative gas of SF_6 to limit the use of SF_6. [3]–[5]. In recent years, $C_5F_{10}O$ has received much attention due to its excellent electrical insulation and environmental performance [6], [7]. At present, most researches on $C_5F_{10}O$ domestic and abroad focus on electrical insulation properties. Preve [5] of Xi'an Jiaotong University evaluated $C_5F_{10}O$ by comparing the thermophysical properties of $C_5F_{10}O$, SF_6, CF_4, CO_2 and N_2 plasmas. Arc extinguishing performance of $C_5F_{10}O$. The local thermodynamic equilibrium components of pure $C_5F_{10}O$ ranged from 300 to 30000 K in the temperature range of 1∼ 10 atm were calculated by the Gibbs free energy minimization method, and the corresponding transport coefficients were calculated by the Chapman-Ensk method. Through comparison of thermal physical properties, it is found that $C_5F_{10}O$ has similar characteristics to SF_6, and the specific heat peak is below 4500 K, which has good thermal interruption capability. However, the 7000 K specific heat peak corresponding to the co-decomposition may reduce the thermal interruption

The associate editor coordinating the review of this manuscript and approving it for publication was Qiang Yang.

capability. The specific heat peak at high temperatures is related to double or triple bond cleavage. Hyrenbach *et al.* [8] studied the thermodynamic properties and internal arc characteristics of $C_5F_{10}O$/dry air and found that $C_5F_{10}O$ and dry air are thermally conductive due to air in the mixed gas. Poor heat conductivity is inferior to SF_6; $C_5F_{10}O$ and dry air are about 30% higher than the pure SF_6 induced by the initial stage of the arc, and the characteristics of the arc continuous combustion stage is no difference from SF_6. Li *et al.* [9] from Wuhan University analyzed the stability and possible decomposition path of $C_5F_{10}O$ from the perspective of density functional theory, and performed the discharge decomposition characteristics of $C_5F_{10}O$. Experimental studies have found that C-C between the carbonyl carbon atom of $C_5F_{10}O$ and the carbon atom at the alpha position is easily broken to form $CF_3CO\cdot$, $C_3F_7\cdot$ Or a free radical such as $C_3F_7C\cdot$, $CF_3\cdot$. Stoler *et al.* [10] studied the insulation and arc-extinguishing properties of $C_5F_{10}O/O_2/CO_2$ mixed gas. The results show that the electrical insulating ability of the mixed gas is very similar to that of SF_6 gas. However, the arc extinguishing ability cannot act as good as that of SF_6 gas. ABB has conducted extensive research on the insulation and arc extinguishing performance of $C_5F_{10}O$ and CO_2 or air mixed gas [11]–[13], and considers $C_5F_{10}O$ in medium and low pressure gas insulation. The equipment has the potential to replace SF_6 gas, and developed a 22kV ring network switchgear with $C_5F_{10}O$/air mixed gas as insulation medium, and commissioned in a substation in Zurich in 2015 [14]. The above research work lays a solid foundation for $C_5F_{10}O$ instead of SF_6 and engineering application.

However, in the engineering application of $C_5F_{10}O$ gas, there will be a frequent fault called local over-thermal fault (POF) that often occurs inside the equipment. Under the long-term effect of POF, whether $C_5F_{10}O$ itself can continue to be stable and keep its insulating performance is another important factor determining its engineering application, and the stability of $C_5F_{10}O$ gas insulating medium at local high temperature has not been confirmed by experiments. Therefore, this paper investigates the stability of $C_5F_{10}O/CO_2$ mixed gas under the action of POF through systematic experiments. The experimental system studies the $C_5F_{10}O$ gas insulating medium under the action of POF, the relationship between the temperature at which decomposition occurs, the initial temperature at which each product is produced, the amount of each product produced. POF temperature and these experimental results will lay the foundation for the subsequent application of $C_5F_{10}O$.

II. $C_5F_{10}O$ OVER THERMAL EXPERIMENT

The experiment in this paper is carried out on the experimental system shown in Fig.1. The POF physical defect model is shown in Fig.2. The detection system uses the Shimadzu QP2010 Ultra Gas Chromatography/Mass Spectrometer (GC/MS) for qualitative and quantitative determination of the decomposed components. Among them, the gas chromatograph uses high-purity He (purity 99.999%)

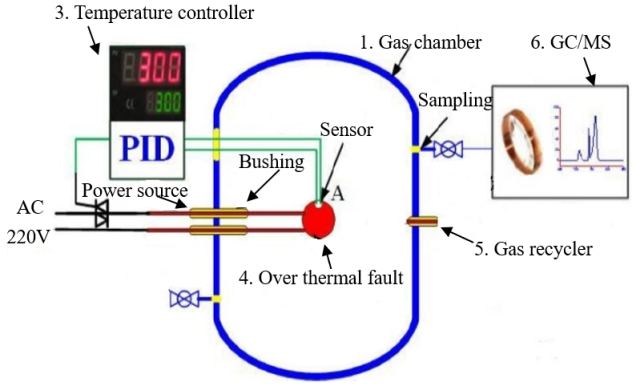

FIGURE 1. The experimental system structure.

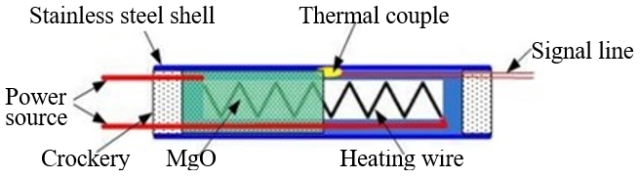

FIGURE 2. The physical defect model and structure of POF Simulation.

as carrier gas, and adopts special capillary column (CP-Sil5CB 60mtr×0.32mm). Its working conditions are: flow rate 2ml/min, oven temperature constant 30°, split ratio 10:1, under these conditions, CF_4, C_2F_6, C_2F_4, C_3F_8, C_5F_{12}, C_3F_6, COF_2, CO, CO_2 and other major decomposition component gases can be effectively separated and detected. Till now, among all decomposition component gases which are scanned by GC/MS, only CF_4, C_2F_6, C_3F_8 and C_3F_6 can be quantitative detected due to the limit of standard gases. So in this paper, only the concentration characteristics of these 4 decomposition products are analyzed. The main functions and design principles of each part of the experimental system have been described in detail in [15] and will not be described here.

In order to eliminate the influence of the ambient temperature on the experimental results, the laboratory temperature was controlled at 20° and the relative humidity was controlled at 50%. All experiments were carried out under these conditions. The specific steps are as follows:

A. STEP 1

Connect the test system and check the air-tightness of the air chamber. The air chamber was scrubbed with absolute ethanol, and then the closed air chamber was evacuated by a vacuum pump to check the airtightness of the air chamber.

B. STEP 2

Air chamber cleaning. The chamber was evacuated, vacuumed and charged with 0.1MPa CO_2 fresh gas, and then vacuumed again, and this process will be repeated twice. After the last vacuuming, according to the partial pressure

ratio, first fill 5% of $C_5F_{10}O$, then after immersing 95% CO_2 to 0.2MPa, let stand for 12 hours, so that the gas is thoroughly mixed.

C. STEP 3

Collect gas samples and component analysis. Under a given temperature condition, $C_5F_{10}O$ is used to decompose the sample gas from the gas outlet every 1 hour, and the sample components are quantitatively analyzed by GC/MS to obtain at different POF temperatures, localized over thermal decomposition characteristics of $C_5F_{10}O$.

D. STEP 4

The experiment is over. After 10 hours, when all the indicators of the experiment were tested, the POF physical defect model was replaced, the chamber was vacuumed, stay for 24 hours, so that the impurity components adsorbed on the wall and the hot electrode surface were fully released. This can reduce the impact on the next set of experiments. At last, return to step 1 and proceed to the next set of tests.

In step 2, mixed gas is 5% $C_5F_{10}O$, and 95% CO_2 at 0.2MPa in this experiment. This ratio can maintains the mixed gas as gas state, in the meantime, keeps a good insulation performance. Other proportions of gas mixtures are in our future plan.

In step 3, during every single experiment, the over thermal temperature is set to a fixed value between 375°C ∼525°C, because our current experimental conditions could reach the highest heating point temperature as 525°C. Then we decreased the fault temperature by 25°C for each experiment, until $C_5F_{10}O/CO_2$ mixed gas does not generate any decomposition products. At 375°C, no decomposition products were detected steadily.

III. EXPERIMENTAL RESULTS AND ANALYSIS

A. EXPERIMENTAL RESULTS

The over thermal experiment results from 150°C to 525°C showed that the mixture of 5% $C_5F_{10}O$ and 95%CO_2 with a gas pressure of 0.2 MPa did not decompose when the POF temperature was lower than 375°C. It is higher than the initial decomposition temperature (260°C) of SF_6 gas under the same conditions [16]; when $C_5F_{10}O$ starts to decompose, the most easily produced product is C_3F_8 and C_3F_6, starting at about 400°C at POF temperature, while CF_4 is produced as a stable product at 500°C, C_2F_6 at 525°C. The initial generation temperatures of the main decomposition products are shown in Table 1. More decomposition opponents are scanned by GC/MS over 525°C as shown in Fig.3, and four of them can be quantitative detected.

Fig.4 is a plot of CF_4 gas concentration as a function of local overheat fault temperature and fault duration. It can be seen from Fig.3 that CF_4 begins to exist as a stable decomposition product when the superheat temperature exceeds 500°C. The concentration of CF_4 increases with the pro-longed duration of failure and is positively correlated with the fault temperature. The highest concentration of CF_4 was 6.42 ppm over the experimental temperature range. As shown in Fig.5, C_2F_6 only C_2F_6 can be decomposed after the local over thermal temperature gets over 525°C. After 10 hours of continuous over thermal, the amount of formation is 17.6 ppm.

In addition, it has been found through repeated experiments that both CF_4 and C_2F_6 are decomposition products of $C_5F_{10}O$ gas insulating medium which decompose after the fault temperature is higher than 500°C. The maximum temperature range of the hot spot can be roughly judged by detecting the presence or absence of CF_4 or C_2F_6.

TABLE 1. Variation table of component concentration under different fault temperature and their initial generative temperatures.

Product	CF_4	C_2F_6	C_3F_8	C_3F_6
Initial generation temperature	500	525	400	400
Concentration(400℃, 10h)	--	–	2.04	50.3
Concentration(525℃, 10h)	6.42	17.6	31.9	190

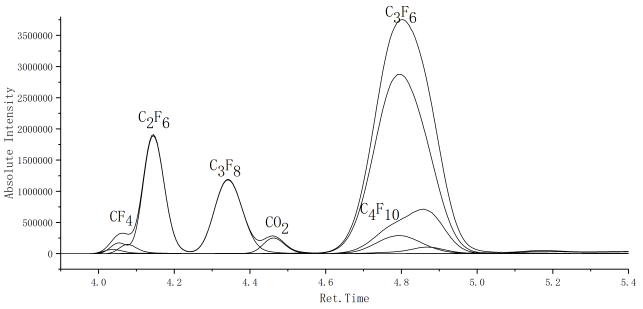

FIGURE 3. GC/MS scanned decomposition opponents.

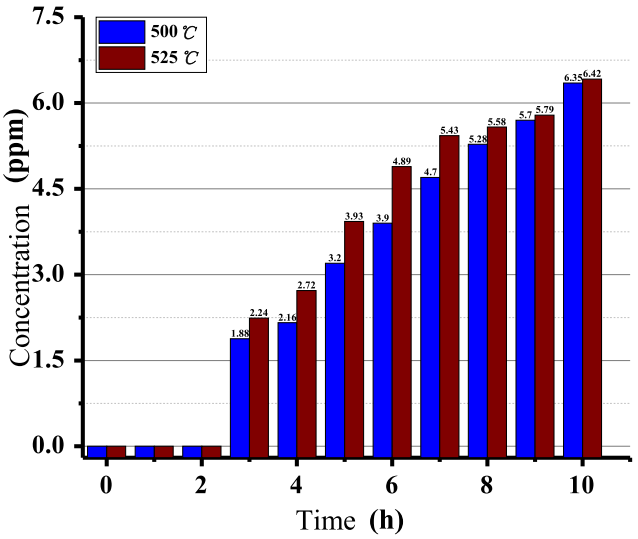

FIGURE 4. The graph of the relationship between the concentration of CF_4 and the fault temperature or time.

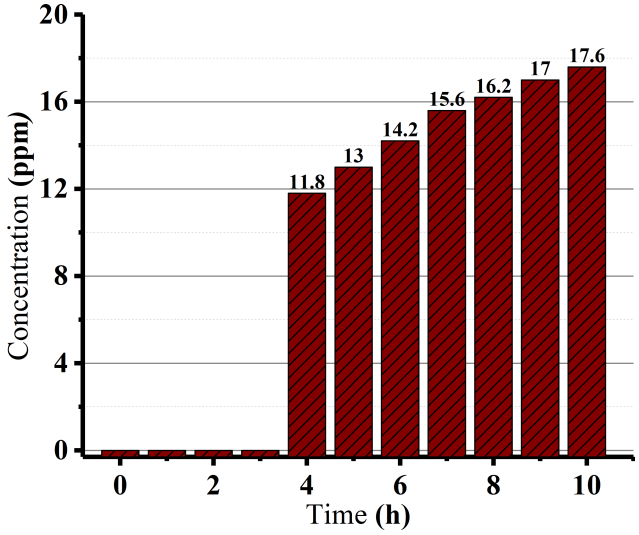

FIGURE 5. The graph of the relationship between the concentration of C_2F_6 and the fault temperature or time.

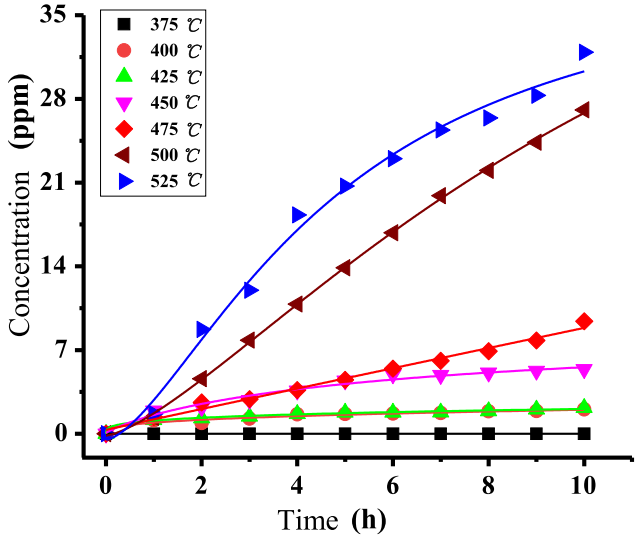

FIGURE 6. The curve of the relationship between the concentration of C_3F_8 and the fault temperature or time.

The $C_5F_{10}O$ gas insulating medium begins to decompose at a fault temperature of 375°C, and mainly generates C_3F_8 and C_3F_6, and Fig.6 shows C_3F_8 generation curve and characteristic curve of fault temperature and fault duration. At a failure temperature of 400°C, $C_5F_{10}O$ decomposed for one hour to produce approximately 1.12 ppm of C_3F_8. As the fault temperature increases, the rate of $C_5F_{10}O$ decomposing to form C_3F_8 is increasing, especially when the fault temperature exceeds 500°C, $C_5F_{10}O$ decomposition produces a significant change in the rate of C_3F_8, which exacerbates the decomposition of $C_5F_{10}O$.

Fig.7 is a characteristic curve of $C_5F_{10}O$ decomposed to generate C_3F_6 under different fault temperature and fault duration. Similar to C_3F_8, the amount of C_3F_6 produced

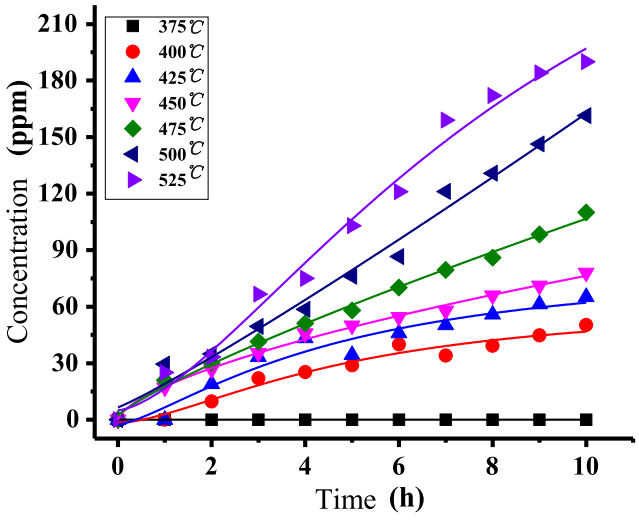

FIGURE 7. The curve of the relationship between the concentration of C_3F_6 and the fault temperature or time.

has a strong positive correlation with the fault temperature and duration. The higher the overheat fault temperature, the higher the rate of $C_5F_{10}O$ decomposing to C_3F_6, and C_3F_6 is the component with the highest rate of formation among all decomposition products, at 525° up to about 190ppm.

In general, as the temperature of local over thermal fault increases, $C_5F_{10}O$ will gradually decompose and generate products such as CF_4, C_2F_6, C_2F_4, C_3F_8, C_5F_{12}, C_3F_6, COF_2, CO and CO_2. At lower temperatures, the formation rate of each component is relatively small. as the temperature increases, the rate of formation of each product increase, but the degree of growth varies greatly depending on the type of product, among those 4 products that can be quantitatively detected, specifically: C_3F_6 >C_3F_8 > C_2F_6 >CF_4. Over these four decomposition products, the smallest concentration is CF_4 within 10 ppm, the amount of C_3F_6 produced is up to 190 ppm. In particular, CF_4 and C_2F_6 are decomposition products of $C_5F_{10}O$ which can be produced after the failure temperature is higher than 500°. C_3F_6, C_3F_8 are the two decomposition components that are most easily generated and produced by $C_5F_{10}O$ decomposition. Therefore, C_3F_6 and C_3F_8 can be used as the main feature for characterizing the thermal decomposition of $C_5F_{10}O$ insulating medium.

B. ANALYSIS OF EXPERIMENTAL RESULTS

According to the frontier molecular orbital theory, the energy difference (energy gap value) of the highest energy unoccupied molecular orbital (HUMO) and the lowest energy unoccupied molecular orbital (LUMO) in the molecular orbital It reflects the ability of electronic transitions to empty orbits. The larger the energy gap, the harder it is for electronic transitions and the more stable the molecular chemical properties. The calculation results in [7] show that the wave function of the frontier molecular orbital is mainly distributed on the carbonyl (C=O) carbon atom and its adjacent carbon atoms,

and the carbon-oxygen double bond has the highest reactivity. Molecular orbital theory indicates that the positions with high charge density on HUMO and LUMO are prone to reactions. The molecule absorbs energy at high temperatures produces free radical particles, and the possible reaction paths are shown in Table 2. In Table 2, the decomposition paths 1 and 2 correspond to the process of C-C bond breaking between carbonyl carbon atoms and alpha carbon atoms in $C_5F_{10}O$ molecule structure to form free radicals, in which the energy absorbed by path 1 is 397.322 kJ/mol, which is higher than that of path 2, 327.989 kJ/mol; path 3 corresponds to the breaking of carbonyl beta carbon atoms in $C_5F_{10}O$ molecule and the C-C bond between the carbonyl beta carbon atoms and the carbon atoms The process requires absorption of 293.258 kJ/Mol.

TABLE 2. Possible decomposition paths of $C_5F_{10}O$.

Reaction path	Chemical equation	Reaction energy(kJ/mol)
1	$(CF_3)_2CFCOCF_3 \rightarrow C_3F_7CO\cdot + CF_3$	397.32
2	$(CF_3)_2CFCOCF_3 \rightarrow CF_3CO\cdot + C_3F_7\cdot$	327.99
3	$(CF_3)_2CFCOCF_3 \rightarrow CF_3\cdot + CF_3CFCOCF_3\cdot$	293.26
4	$(CF_3)_2CFCOCF_3 \rightarrow CF_3CO\cdot + C_3F_7 + e$	1123.9
5	$(CF_3)_2CFCOCF_3 \rightarrow C_3F_7CO\cdot + CF_3 + e$	1166.6
6	$C_3F_7CO\cdot \rightarrow C_3F_7\cdot + CO$	21.357
7	$CF_3CO\cdot \rightarrow CF_3\cdot + CO$	33.779
8	$CF_3CFCOCF_3\cdot \rightarrow CF_3\cdot + CF_3CFCO\cdot$	194.48
9	$CF_3CFCOCF_3\cdot \rightarrow CF_3CF\cdot + COCF_3\cdot$	367.55

Lastly, free radicals produced by ionization or dissociation of $C_5F_{10}O$ molecule have strong reactivity and can produce a series of new substances such as CF_4, C_2F_6, C_3F_8, C_3F_6, C_4F_{10}, C_5F_{12}, C_6F_{14} [17] through secondary reactions, as shown in Table 3.

TABLE 3. Possible pathways of decomposition products.

Reaction path	Chemical equation	Reaction energy(kJ/mol)
1	$CF_3\cdot + F\cdot \rightarrow CF_4$	-527.99
2	$2CF_3\cdot \rightarrow C_2F_6$	-370.58
3	$C_3F_7\cdot + F\cdot \rightarrow C_3F_8$	-464.01
4	$C_3F_7\cdot \rightarrow C_3F_6 + F\cdot$	230.81
5	$CF_3\cdot + C_3F_7\cdot \rightarrow C_4F_{10}$	-423.64
6	$C_3F_7\cdot + 2CF_3\cdot \rightarrow C_5F_{12} + F\cdot$	-258.29
7	$2C_3F_7\cdot \rightarrow C_6F_{14}$	-327.16

The chemical reactions that generate CF_4, C_2F_6 and C_3F_8 are all exothermic reactions, and the reaction to form C_3F_6 is endothermic. So under the action of over thermal fault, the generation of C_3F_6 is extremely advantageous. Therefore, $C_5F_{10}O$ is most easily to generate C_3F_6, and its amount

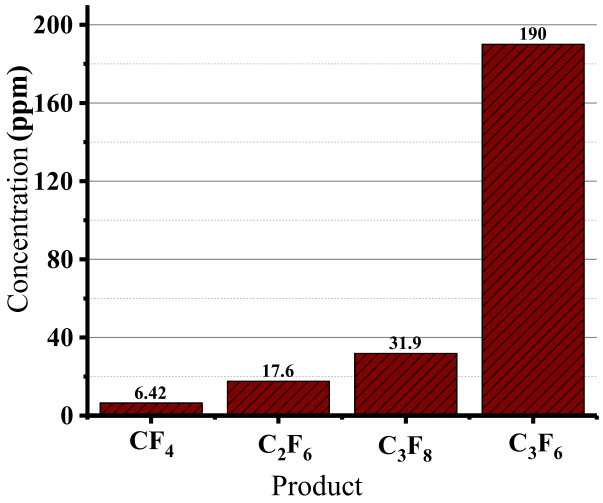

FIGURE 8. The decomposition of components of $C_5F_{10}O$ after 10 hours' fault at 525°.

produced is also the largest among these four decomposition products.

C. ANALYSIS OF CHARACTERISTIC COMPONENT GENERATION RATE

The analysis in the last two sections obviously shows that in the overheat fault interval (375°C ~ 525°C), C_3F_6 and C_3F_8 are the most able to characterize $C_5F_{10}O$ over thermal, and can be the main characteristic component of decomposition. This section will further reveal the thermal decomposition characteristics of $C_5F_{10}O$ by the generation rate of C_3F_6 and C_3F_8. The $C_5F_{10}O$ mixed gas provides the basis for fault monitoring of gas insulated equipment as the main insulating medium.

Since the experimental single data points are susceptible to other variables such as air pressure, $C_5F_{10}O/CO_2$ ratio, it is difficult to accurately describe the $C_5F_{10}O$ mixed gas and the law of thermal decomposition of insulating medium. However, if all valid data at the same fault temperature is reconstructed, such as linear fitting of the characteristic data of the previous section, roughly obtain C_3F_6 and C_3F_8, the relationship between the generation rate and the overheat fault temperature is shown in Fig.9 and Fig.10.

Fig.9 and Fig.10 show that C_3F_6 and C_3F_8 have significant changes in the rate of formation and a strong linear positive correlation with the over thermal temperature. The generation rates of C_3F_6 and C_3F_8 at different failure temperatures are listed in Table 4. At 400°C, the rate of formation of C_3F_8 is about 0.114 ppm/h, at 525° is 2.854 ppm/h; C_3F_6 is most productive among all the four products, about 4.982 ppm/h at 400°C, 20.75 ppm/h at 525°C.

Fig.11 is a graph that shows the relationship between the generation rate of C_3F_6 and C_3F_8 and the over thermal fault temperature. It can be seen from Fig.10 that the generation rates of C_3F_6 and C_3F_8 gradually increase with increasing temperature, are basically exponential. When the $C_5F_{10}O$

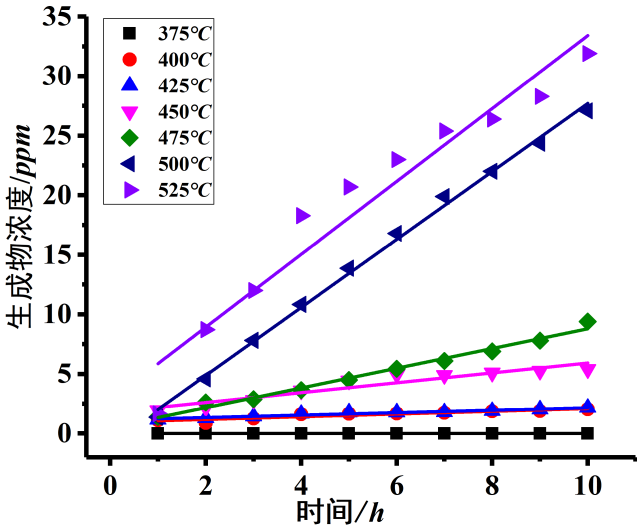

FIGURE 9. Generation characteristics of C_3F_6 at different fault temperatures.

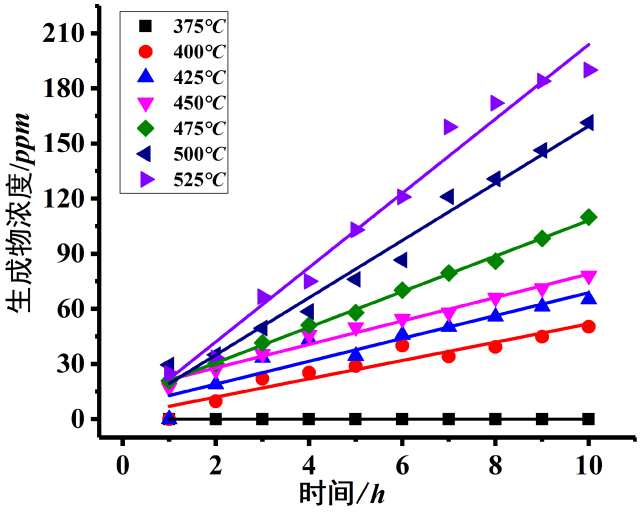

FIGURE 10. Generation characteristics of C_3F_8 at different fault temperatures.

TABLE 4. Production rate of C_3F_8 and C_3F_6 in different temperature.

Overheat fault temperature /°C	C_3F_8 gas production rate (ppm/h)	C_3F_6 gas production rate (ppm/h)
400	0.114	4.982
425	0.103	6.219
450	0.415	6.384
475	0.828	9.71
500	2.854	15.636
525	3.059	20.75

mixed gas is used in industry in the future, the internal decomposition rate of the two internal decomposition components: C_3F_6 and C_3F_8 can be utilized, to make a more accurate assessment of the extent of the failure.

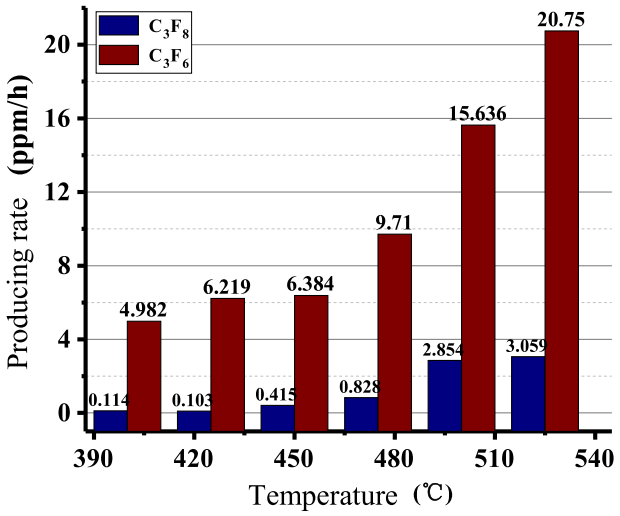

FIGURE 11. Correlation picture between characteristic component formation rate and fault temperature.

IV. CONCLUSION

1) Through repeated experiments, it is found that a 0.2MPa 5% $C_5F_{10}O$ and 95% CO_2 mixed gas insulating medium begins to decompose at about 375°C, producing C_3F_8 and C_3F_6, and generates CF_4, C_2F_6, C_2F_4, C_5F_{12}, COF_2, CO, CO_2 and other components at higher temperature. Under the same conditions, the thermal stability is better than that of SF_6 gas insulating medium from the decomposition starting temperature.
2) Among the components generated by $C_5F_{10}O$ over thermal decomposition, the heated state is extremely favorable for the generation of C_3F_6 because it is an endothermic reaction. Therefore, $C_5F_{10}O$ is most likely to generate C_3F_6 when it is decomposed under the action of over thermal fault, and its amount is also the largest among those four quantitatively detected decomposition products. In contrast, the chemical reactions that generate C_2F_6 and CF_4, and C_3F_8 are exothermic reactions, especially C_2F_6 and CF_4. So the formation is hard and requires a higher reaction temperature (about 500°C).
3) The increase of fault temperature will aggravate the decomposition of $C_5F_{10}O$, and accelerate the formation of C_3F_8, C_3F_6, C_2F_6. The formation of components such as CF_4, due to the difference in the reaction properties of the respective decomposition components, causes the failure temperature to have different effects on the rate of formation of each decomposition component.
4) $C_5F_{10}O$ most easily generates C_3F_8 and C_3F_6 in condition of over thermal fault. The generation characteristics of C_3F_8 and C_3F_6 can be the main feature quantities for characterizing the thermal state of $C_5F_{10}O$ insulating medium. In the future industrial

application of $C_5F_{10}O$ mixed gas, the degree of over thermal failure of the equipment can be estimated by the formation rate of C_3F_8 and C_3F_6 or their assessed development trends.

REFERENCES

[1] H. Koch and M. Hopkins, "Overview of gas insulated lines (GIL)," *J. IEEE Power Energy Mag.*, vol. 3, no. 2, pp. 940–944, Jun. 2005.
[2] Y. Deng, M. Yi, and X. Chen, "A review on the research progress of sulfur hexafluoride alternative gases," *J. Yunnan Electric Power Technol.*, vol. 2, pp. 45–85, Aug. 2017.
[3] B. Wu, L. Shu, and W. Sima, "SF6 gas insulation and earth greenhouse effect," *J. High Voltage Aparatus*, vol. 36, no. 6, pp. 23–26, May 2000.
[4] Z. Xiang *et al.*, "Reducing sulfur hexafluoride emission to address global climate change," *Chin. J. Environ. Manage.* vol. 2, pp. 23–27, May 2010.
[5] C. R. D. Preve, "Method for validation of new eco-friendly insulating gases for medium voltage equipment," in *Proc. IEEE Int. Conf. Dielectr. (ICD)*, Jul. 2016, pp. 235-240.
[6] Y. Wu *et al.*, "Evaluation of SF6-alternative gas C5-PFK based on arc extinguishing performance and electric strength," *J. Phys. D, Appl. Phys.*, vol. 50, p. 38, Jul. 2017.
[7] X. Li, H. Zhao, and A. B. Murphy, "SF6 alternative gases for application in gas-insulated switchgear," *J. Phys. D, Appl. Phys.*, vol. 51, no. 15, Mar. 2018, Art. no. 153001.
[8] M. Hyrenbach *et al.*, "Alternative insulation gas for medium-voltage switchgear," in *Proc. Petroleum Chem. Ind. Conf. Eur. (PCIC Europe)*, Jun. 2015, pp. 1–9.
[9] Y. Li *et al.*, "Decomposition mechanism of $C_5F_{10}O$: An environmentally friendly insulation medium," *Environ. Sci. Technol.*, vol. 38, no. 14, pp. 10127–10136, 2017.
[10] P. Stoller, C. Doiron, and C. D. Tehlar, "Mixtures of CO_2 and $C_5F_{10}O$ per fluoroketone for high voltage ap-plications," *IEEE Trans. Dielectr. Elect. Insul.*, vol. 24, no. 5, pp. 2712–2721, Jul. 2017.
[11] Y. Kieffel and F. Kieffel, "SF6alternative development for high voltage switchgears," in *Proc. IEEE Elect. Insul. Conf. (EIC)*, Jun. 2015, pp. 379-383.
[12] M. Hyrenbach and S. Zache, "Alternative insulation gas for medium-voltage switchgear," in *Proc. Petroleum Chem. Ind. Conf. Eur. (PCIC Europe)*, Jun. 2015, pp. 1–5.
[13] J. D. Mantilla, N. Gariboldi, S. Grob, and M. Claessens, "Investigation of the insulation performance of a new gas mixture with extremely low GWP," in *Proc. IEEE Elect. Insul. Conf. (EIC)*, Jun. 2014, pp. 469–473.
[14] H. Maik and S. Zache, "Alternative gas insulation in medium-voltage switchgear," in *Proc. Petroleum Chem. Ind. Conf. Eur.*, Jun. 2015, pp. 15–18.
[15] F. Zeng, "Characteristics of SF6 under partial over-thermal fault and the influence mechanism of trace H_2O," Ph.D. dissertation, 2014.
[16] F. Zeng *et al.*, "Decomposition characteristics of SF_6 under thermal fault for temperatures below 400ÂřC," *IEEE Trans. Dielectr. Electr. Insul.*, vol. 21, no. 3, pp. 995–1004, Jun. 2014.
[17] A. V. Tatarinov *et al.*, "Dielectric barrier discharge processing of trans-$CF_3CH{=}CHF$ and $CF_3C(O)CF(CF_3)_2$, Their Mixtures with Air, N_2, CO_2 and analysis of their decomposition products," *J. Plasma Chem. Plasma Process.*, vol. 35, no. 5, pp. 845–862, Sep. 2015.

FUPING ZENG was born in Chongqing, China, in 1984. He received the B.S. degree in electrical engineering from Dalian Maritime University, the M.S. and Ph.D. degrees from Chongqing University, and the master's degree from Wuhan University, China, where he is currently a Professor. His research interests include the online monitoring and the fault diagnosis of HV electric equipment insulation.

ZHAOFENG WAN was born in Hohhot, Inner Mongolia, China, in 1995. He received the B.S. degree from the School of Electrical Engineering, Chongqing University, Chongqing, China. He is currently pursuing the master's degree with Wuhan University, China. His research interests include GIS condition monitoring and fault diagnosis.

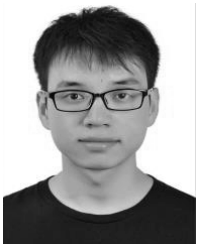

ZHICHENG LEI was born in Fuding, Fujian, China, in 1994. He received the bachelor's degree in electrical engineering from Chongqing University, Chongqing, China. He is currently pursuing the master's degree with Wuhan University, China. His research interests include environmentally friendly insulating gas, and GIS condition monitoring and fault diagnosis.

JU TANG was born in Pengxi, Sichuan, China, in 1960. He received the B.Sc. degree from Xi'an Jiaotong University, and the M.Sc. and Ph.D. degrees from Chongqing University, China.

He is a Professor with Wuhan University, a Professor with the State Key Laboratory of Power Transmission Equipment and System Security and New Technology, Chongqing University, and the Chief Scientist presiding over the National Basic Research Program of China (973 Program) (2009CB724500).

His research interests include the online monitoring and fault diagnosis of HV electric equipment insulation.

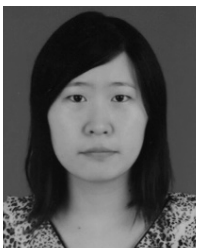

LIANGJUN DAI was born in Qianjiang, Hubei, China, in 1996. She received the bachelor's degree from the College of Electrical Engineering, Chongqing University. She is currently pursuing the master's degree with the School of Electrical and Automation, Wuhan University. Her research interests include the alternative gas of sulfur hexafluoride and the restoration characteristics of heptafluoropropyl trifluorovinyl ether.

XIAOHUA WANG was born in Zhejiang, China, in 1978. He received the B.S. degree from Chang'an University, and the M.S. and Ph.D degrees from Xi'an Jiaotong University. He is currently a Professor with Xi'an Jiaotong University. His research interests are electrical testing and fault diagnosis technology, electrical intelligent theory and technology, and environmental protection switchgear design technology.

QIANG YAO was born in Chongqing, China, in 1971. He received the B.S. and M.S. degrees from Chongqing University, Chongqing, China.

He is currently a Senior Engineer with Chongqing Power Company and is engaged in the analysis of decomposition components of SF_6.